BBA - Bioenergetics 1860 (2019) 201–208

Contents lists available at ScienceDirect

BBA - Bioenergetics

journal homepage: www.elsevier.com/locate/bbabio

Molecular dynamics and structural models of the cyanobacterial NDH-1 complex

Patricia Saura, Ville R.I. Kaila*

Department of Chemistry, Technical University of Munich (TUM), Lichtenbergstraße 4, Garching D-85747, Germany

ARTICLE INFO

Keywords:
Complex I
Proton pumping
Electron transfer
Photosynthesis
Bioenergetics

ABSTRACT

NDH-1 is a gigantic redox-driven proton pump linked with respiration and cyclic electron flow in cyanobacterial cells. Based on experimentally resolved X-ray and cryo-EM structures of the respiratory complex I, we derive here molecular models of two isoforms of the cyanobacterial NDH-1 complex involved in redox-driven proton pumping (NDH-1L) and CO_2-fixation (NDH-1MS). Our models show distinct structural and dynamic similarities to the core architecture of the bacterial and mammalian respiratory complex I. We identify putative plastoquinone-binding sites that are coupled by an electrostatic wire to the proton pumping elements in the membrane domain of the enzyme. Molecular simulations suggest that the NDH-1L isoform undergoes large-scale hydration changes that support proton-pumping within antiporter-like subunits, whereas the terminal subunit of the NDH-1MS isoform lacks such structural motifs. Our work provides a putative molecular blueprint for the complex I-analogue in the photosynthetic energy transduction machinery and demonstrates that general mechanistic features of the long-range proton-pumping machinery are evolutionary conserved in the complex I-superfamily.

1. Introduction

The cyanobacterial NDH-1 complex (type-I NADH dehydrogenase) is a large, ca. 0.5 MDa, enzyme that reduces plastoquinone (PQ) and couples the released free energy to proton pumping across a biological membrane to drive active transport and synthesis of adenosine triphosphate (ATP) [1–3]. NDH-1 is structurally related to respiratory complex I (NADH:ubiquinone oxidoreductase), but unlike the latter, the cyanobacterial enzyme supports cyclic electron flow around photosystem I as well as inorganic carbon uptake via CO_2 [4–6]. NDH-1 is also present in plants and algae that harbor the respiratory and photosynthetic machineries in their mitochondria and chloroplasts, respectively. Both energy conversion chains, however, co-exist in the thylakoid and cytoplasmic membranes of cyanobacteria, while the cyanobacterial NDH-1 has evolved distinct features to interact with both respiratory and photosynthetic enzymes [2,3,7]. Despite recent advances in structural [8–14] and mechanistic [15–19] understanding of the respiratory complex I, we still lack a detailed molecular and functional picture of the cyanobacterial NDH-1 complex.

Biochemical studies [20] suggest that NDH-1 is expressed in different isoforms. The NDH-1L and NDH-1L′ isoforms support respiration and cyclic electron flow, whereas NDH-1MS and NDH-1MS′ are involved in CO_2 uptake. Moreover, the NDH-1L′ and NDH-1MS′ isoforms are constitutive, whereas the NDH-1L and NDH-1MS isoforms are expressed under low CO_2 concentrations [21]. All NDH-1 isoforms contain a hydrophilic domain with subunits NdhI/J/K/H harboring three iron-sulfur (FeS) centers, N6a, N6b, and N2 [1]. However, in contrast to the respiratory complex I, which receives electrons from NADH via FMN across a ca. 100 Å-long chain of 8–9 FeS centers [22,23], ferredoxin has been suggested to bind to subunit NdhS, and provide electrons directly to the N6a center [24]. Moreover, in contrast to complex I, which employs ubiquinone [25] or menaquinone [26], the NDH-1 complex operates with plastoquinone [2].

The proton pumping subunits of NDH-1 are located in the membrane domain of the enzyme, and comprise subunits NdhA, NdhC, NdhE, NdhG, in addition to NdhB, NdhD1 (D2), and NdhF1 in the NDH-1L (NDH-1L′) isoform (Table S1). Subunits NdhB, NdhD, and NdhF are homologous to the antiporter-like subunits Nqo14 (NuoN/ND2; *T. thermophilus/E. coli*/bovine numbering), Nqo13 (NuoM/ND4), and Nqo12 (NuoL/ND5), and are likely to provide key parts of the proton pumping machinery [1] (Table S1). Interestingly, the NDH-1MS and NDH-1MS′ variants express different terminal NdhD3 (NdhD4) and NdhF3 (NdhF4) subunits, which further bind to the CupA, CupB, and CupS subunits, responsible for the CO_2 uptake and fixation [27].

To obtain structural insight into NDH-1, we derive here molecular models of two NDH-1 isoforms involved in redox-driven proton pumping (NDH-1L) and CO_2-fixation (NDH-1MS) based on recently

* Corresponding author.
E-mail address: ville.kaila@ch.tum.de (V.R.I. Kaila).

https://doi.org/10.1016/j.bbabio.2018.11.010
Received 13 September 2018; Received in revised form 30 October 2018; Accepted 7 November 2018
Available online 16 November 2018

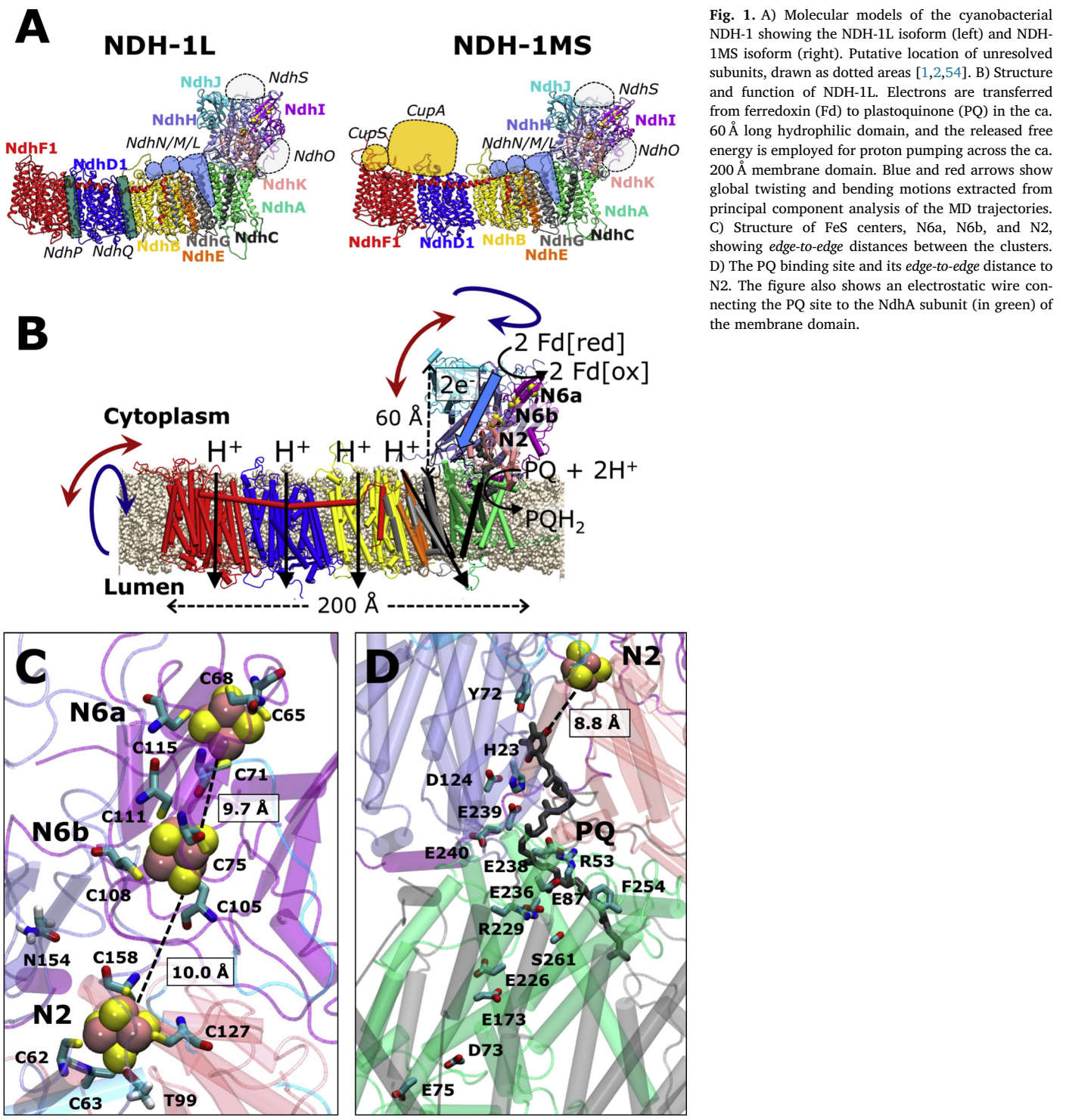

Fig. 1. A) Molecular models of the cyanobacterial NDH-1 showing the NDH-1L isoform (left) and NDH-1MS isoform (right). Putative location of unresolved subunits, drawn as dotted areas [1,2,54]. B) Structure and function of NDH-1L. Electrons are transferred from ferredoxin (Fd) to plastoquinone (PQ) in the ca. 60 Å long hydrophilic domain, and the released free energy is employed for proton pumping across the ca. 200 Å membrane domain. Blue and red arrows show global twisting and bending motions extracted from principal component analysis of the MD trajectories. C) Structure of FeS centers, N6a, N6b, and N2, showing *edge-to-edge* distances between the clusters. D) The PQ binding site and its *edge-to-edge* distance to N2. The figure also shows an electrostatic wire connecting the PQ site to the NdhA subunit (in green) of the membrane domain.

resolved experimental structures of complex I [8–11]. In order to gain mechanistic insight of NDH-1, we study the dynamics of these enzymes in a biological lipid membrane-water environment using large-scale atomistic molecular dynamics (MD) simulations.

2. Methods

2.1. Structural modeling

The structure of the cyanobacterial NDH-1 complex was built by homology modeling, using Modeller 9.19 [28] based on the amino acid sequence of the *Synechocystis* sp. PCC 6803 NDH-1 (Table S6). Experimentally resolved structural templates were identified using the HHPred server (https://toolkit.tuebingen.mpg.de/#) and compared to query sequences within the Protein Data Bank database. Complex I from *Thermus thermophilus* (PDB ID: 4HEA) [8]; *E. coli* (PDB ID: 3RKO) [10]; *Ovis aries* (PDB ID: 5LNK) [9], and *Bos taurus* (PDB ID: 5LC5) [11] were used as experimental templates for the NDH-1 models. The relative position, orientation, and subunit contacts of the different monomers in the NDH-1 model, were based on the *Thermus thermophilus* crystal structure of the complete respiratory complex I (PDB ID: 4HEA, Fig. 1). No well-conserved structural templates were found for NdhL/

M/N/O/P/Q/S, and CupA/B (see Table S1), and were therefore not included in the structural models. Multiple sequence alignments were performed with Clustal Omega [29], and identified homology to complex I is shown in Table S1. The three FeS cofactors, N6a, N6b, and N2, as well as the PQ substrate were modeled based on previous work [16–18], and by using distance restrains between the Fe atom and the protein cysteine residues of the first coordination sphere. The PQ was built after the structural modeling in the PQ-cavity identified using HOLE [30], and relaxed as described below. The sequence conservation between NDH-1 and the respiratory complex I varies between ca. 30–50%, providing a good basis for the structural modeling (Tables S4, S5, Fig. S13). Regions with higher structural uncertainty are shown in Fig. S2 and structural validation analysis in Table S7 and Fig. S12.

2.2. Molecular dynamics simulations

The dynamics of the derived structural models were studied by atomistic molecular dynamics (MD) simulations. Hydrogen atoms were modeled by assuming standard protonation states, with the exception of residue $His23_H$ in the PQ-binding site, which was modeled in its protonated state due to its ion-pair with $Asp124_H$ (see above). The NDH-1L complex was embedded in a POPC lipid membrane, and solvated with TIP3P water molecules and 100 mM NaCl. The total system comprised ca. 600,000 atoms. MD simulations were performed at $T = 310$ K and $p = 1$ bar in an *NPT* ensemble using the CHARMM36 force field [31] and in-house parameters [16–18] derived based on density functional theory (DFT) calculations for PQ and the FeS centers. Long-range electrostatic interactions were described by the Particle Mesh Ewald (PME) method. The system was gradually relaxed with harmonic restraints of 1–10 kcal mol^{-1} $Å^{-1}$ during the first 5 ns, followed by 10 ns equilibration without restraints. During the initial equilibration steps, the PQ was modeled in its reduced state (PQ^{2-}), followed by modeling of the neutral PQ, that was employed for subsequent MD production steps. A time step of 1 fs was employed during the initial relaxation, whereas a 2 fs time step was used during the production run. MD simulations were performed with NAMD2 [32], and the trajectories were analyzed with VMD [33]. Principal component analysis (PCA) was performed on the MD trajectories using ProDy [34].

3. Results and discussion

3.1. Structure and dynamics of the hydrophilic domain

The structural models of NDH-1 show a global architecture that closely resembles the respiratory complex I [8,9,11,12] (Fig. 1A). The enzymes comprise a hydrophilic domain that harbors the FeS centers and a PQ binding site that are connected to a ca. 200 Å wide membrane domain. In molecular dynamics simulations, the hydrophilic and membrane domains undergo global twisting and bending motions, where the NdhA/K subunits act as a hinge (Figs. 1B, S1). We recently linked similar dynamical motions to the *active-to-deactive* (A/D)-transition in the mammalian enzyme [9,11,35], that strongly modulates the enzyme turnover ([36] and refs. therein). Although it is possible that similar conformational transitions could also regulate the activity of the cyanobacterial enzyme (cf. also [37]), recent structural studies suggest that the yeast complex I is rather rigid [38], and the motions coupled to the A/D transition might not be universally conserved amongst the complex I superfamily. The functional importance of the global motions observed in the MD simulations of the cyanobacterial NDH-1 complex therefore remains unclear.

The hydrophilic domain of the NDH-1 comprises subunits NdhH/I/J/K, NdhO, and NdhS that extend ca. 60 Å above the membrane plane (Fig. 1B), form the PQ-binding site, and harbor the three FeS cofactors, N6a, N6b, and N2 (Fig. 1C, D). NdhS is homologous to the Src homology 3 domain-like fold found in the ferredoxin-binding site of PSI [39,40], and it may thus mediate binding of the electron donor ferredoxin to NDH-1 [2,24,41]. The NdhO subunit may stabilize NdhI and NdhK, and enhance cyclic electron transport activity under high light conditions [42]. The NdhS and NdhO, however, lack structural templates and could not be accurately modeled, why we expect some structural uncertainty in this region (Fig. S2).

The three FeS centers are separated by ca. 10 Å from each other and the terminal N2 center is located ca. 9 Å from the PQ headgroup. This suggests that the electron transfer across the FeS chain takes place on sub-microsecond timescales based on electron transfer theory, and by assuming generic electron transfer parameters [43] (Table S2). In respiratory complex I, the electrons are transferred, one at the time, from NADH to N2 on ca. 90 μs timescales [22,44], whereas the electron transfer process in NDH-1 is likely to be kinetically limited by the diffusion of ferredoxin. This could provide a good starting point to trap the transient plastosemiquinone ($PQ^{-/}\cdot$) intermediate in NDH-1 in contrast to the respiratory complex I, where observation of such intermediate species has been challenging ([15,45,46] but cf. also [47]). The N6a center coordinates to $Cys65_I$, $Cys68_I$, $Cys71_I$, and $Cys115_I$ of NdhI, but we also identify an additional cysteine residue, $Cys119_I$, in the vicinity of the cluster that is conserved in cyanobacteria and higher plants, but not present in the respiratory complex I (Fig. S3). Due to this structural vicinity, it is possible that $Cys119_I$ could replace one of the other cysteine ligands of N6a. The N6b center binds to $Cys75_I$, $Cys105_I$, $Cys108_I$, and $Cys111_I$ of NdhI in the structural models, whereas the terminal N2 center is coordinated by a tandem cysteine motif, $Cys62_K$-$Cys63_K$, $Cys127_K$, and $Cys158_K$ to subunit NdhK. Interestingly, the N2 cluster lacks the residues homologous to $Arg83_{Nqo6}$ and $His169_{Nqo4}$ of the respiratory complex I (*Thermus thermophilus* numbering), which are replaced by $Thr99_K$ and $Asn155_H$ in NDH-1 (Fig. 1C). This is expected to downshift the redox potential of N2 in NDH-1 by up to ca. 200 mV based on continuum electrostatic calculations [18] and experiments [48], which places the N2 redox potential close to those of N6a and N6b, at around ca. −300 mV. Moreover, $His169_{Nqo4}$ in the respiratory complex I accounts for the pH-dependence of the N2 cluster [48], and the N2 center is thus predicted to be pH-independent in NDH-1. The PQ-binding site is structurally similar to the respiratory complex I (see below), and PQ is therefore expected to have a low redox-potential of ca. −300 mV in its binding site [18,45]. The redox potential of cyanobacterial ferredoxin is in the ca. −420 mV range [49], i.e., 100 mV lower than the electron donor NADH in complex I. This small redox drop from ferredoxin to N2 may thus help to drive the electrons to PQ, to stepwise reduce PQ via $PQ^{-/}\cdot$ to plastoquinol (PQH_2).

3.2. Structure, binding, and dynamics of plastoquinone

The PQ-cavity is located ca. 20 Å above the membrane plane, forming a tight ca. 40 Å long tunnel that is surrounded by both charged and non-polar residues (Figs. 1D, 2, S4). This cavity forms around subunits NdhI, NdhK, NdhH, and NdhA, and ends near the N2 center at the NdhH/NdhK interface. The nine isoprenoid units completely fill the PQ-tunnel, with the last isoprenoid unit located at the tunnel opening (Fig. S4). The PQ-headgroup remains in contact with the conserved $His23_H$ and $Tyr72_H$ residues during the MD simulations of both the NDH-1L and NDH-1MS, and at ca. 9 Å *edge-to-edge* distance from the N2 cluster (Fig. 2A). The two conserved $His23_H$ and $Tyr72_H$ residues are likely to function as local proton donors in the reduction of PQ to PQH_2 [17,18]. Upon two-electron reduction and proton transfer from $His23_H$ and $Tyr72_H$, we find that PQH_2 moves away from its primary binding site to a location ca. 10 Å from the $Tyr72_H$ (Fig. 2B, see Table S3) [50].

In the PQ state, $His23_H$ forms a tight ion-pair with the conserved $Asp124_H$, but the PQH_2 formation weakens the His/Asp interaction, consistent with simulations on the respiratory complex I [17,50]. A similar His-Asp dissociation has recently been linked with conformational changes in the Nqo8 subunit that resulted in large pK_a-shifts [17]. We find that the $His23_H$/$Asp124_H$ dissociation in NDH-1 causes conformational changes in a conserved network of nearby charged residues

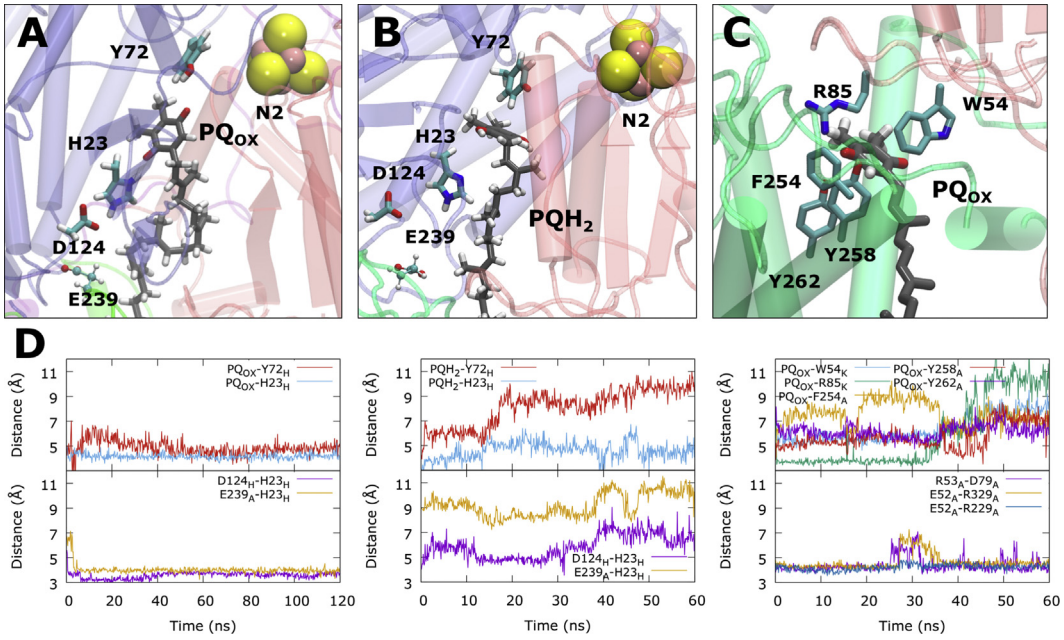

Fig. 2. A) The PQ binding site in NDH-1L with PQ forming contacts to $Tyr72_H$ and $His23_H$. B) Formation of PQH_2 by proton transfer from $Tyr72_H$ and $His23_H$, triggers dissociation of the $His23_H$/$Asp124_H$ ion-pair and leads to dissociation of the PQH_2 (see text). C) PQ at a putative second binding site in the membrane domain forming contacts with $Phe254_A$, $Tyr258_A$, $Tyr262_A$, $Trp54_K$ and $Arg85_K$. D) Distances between functional residues obtained from molecular dynamics simulations in the PQ (left, right panels) and PQH_2 states (middle panel).

(Fig. 4), that propagate to the buried glutamates in the NdhA subunit (Fig. 3), and could link to uptake of protons from the cytoplasmic side via water molecules observed in the MD simulations (see below, Figs. 4, S5). This region is particularly interesting as it forms a hotspot for human disease in the mitochondrial complex I [51,52]. However, there is a structural uncertainty in the NdhA, which may bind to the unresolved NdhN/M/L subunits. Nevertheless, the similar electrostatic-conformational propagation processes in both NDH-1 and the respiratory complex I [17], suggests that the coupling between the electron and proton-transfer units follow overall similar mechanistic principles.

The NDH-1MS isoform shows overall a similar PQ-binding site, but in the MD simulations, $His23_H$ also forms an ion-pair with $Glu239_A$ that competes with $Asp124_H$ (Fig. S6). $Glu239_A$ is located in a glutamate-rich flexible loop, conserved in NDH-1, but it is not present in complex I (see Fig. S7). This region could have a functional role in NDH-1, as it forms contacts with flexible loops of the NdhC and NdhH subunits, and similar regions show structural changes during the A/D-transition in the mammalian complex I [35].

The plastoquinone tunnel bends at ca. 25 Å from the PQ-binding site at $Tyr72_H$/$His23_H$, where we observe several conserved aromatic and charged residues (Table S3). We recently identified a putative second quinone-binding site in this kink region of the bacterial enzyme [50]. In order to probe whether NDH-1 also holds an analogous binding site, we placed a PQ molecule close to this region and performed atomistic MD simulations. During the MD simulations, the PQ headgroup forms contacts with the $Phe254_A$, $Trp54_K$, and a cluster tyrosine residues $Tyr258/262_A$, and $Arg85_K$, suggesting that the putative site is indeed conserved. Importantly, this site is located near conserved glutamates that undergo conformational and protonation changes upon PQH_2 formation (Fig. 2B, see above). Motion of PQ/PQH_2 to this second site has possible mechanistic consequences, as it brings the redox-carrier in the structural vicinity of the proton-pumping elements. Moreover, PQ has a redox potential of ca. +80 mV in membranes [53], suggesting that movement of PQH_2 from its binding site near N2 (ca. −300 mV) towards this membrane-bound loading site couples to energy release, which the enzyme could employ to drive the proton pumping across the membrane. To this end, PQH_2 (or PQH^-, see [15,18]) could push the protons taken up by NdhA towards the antiporter-like subunits, triggering a force propagation cascade across the membrane domain (see below, Fig. 4D).

3.3. The proton-pumping membrane domain

The membrane domain of NDH-1 forms a ca. 200 Å wide module that is clamped together by an 80 Å-long amphipathic HL-helix originating from the NdhF subunit. The membrane domain consists of three homologues antiporter-like subunits, NdhB, NdhD and NdhF, each of which comprise two five-helical bundle segments, TM4-8 and TM9-13, similar as in the respiratory complex I [8]. Moreover, NdhA also contains a highly tilted five-helix bundle segment, TM2-6, that is bridged by subunits NdhC/G/E to NdhB. As mentioned above, NdhA may form additional contacts with NdhL/M/N [54], but these subunits could not be accurately modeled due to lack of structural templates. Interestingly, NdhM resemblances the B13 subunit of the mammalian complex I [20] that was suggested to modulate global motions of complex I [35].

Buried proline and tryptophan residues in the trans-membrane (TM) helices 7 and 12 of NdhB/D/F and TM5 in NdhA induce formation of broken helix-elements (Table S3). These TM helices are dynamically more flexible than the other TM-helices in the MD simulation (Fig. S8), which further allow them to establish proton channels (see below) [16,55]. Each of the antiporter-like subunits, NdhB/D/F in the NDH-1L isoform contain a Lys/Glu ion-pair in TM7 and TM5, respectively, a middle Lys in TM8, and bridging His (NdhD/F) or Gln (NdhB) in TM7, and a terminal Glu or Lys residue in TM12 (Figs. 3, 4). These residues establish the central proton pumping machinery in NDH-1 (see below), and provide thus good candidates for site-directed mutagenesis experiments (Table S3).

NDH-1L and NDH-1MS express different isoforms of the NdhD and NdhF subunits. In NDH-1L, NdhP and NdhQ, may additionally bind to the NdhF1/D1 and NdhD1/B interfaces, respectively, stabilizing the complex [56–59]. Although these single TM subunits (Fig. S9) could not be accurately modeled, we note that they are likely to be located in positions that form putative lipid binding-sites in the respiratory

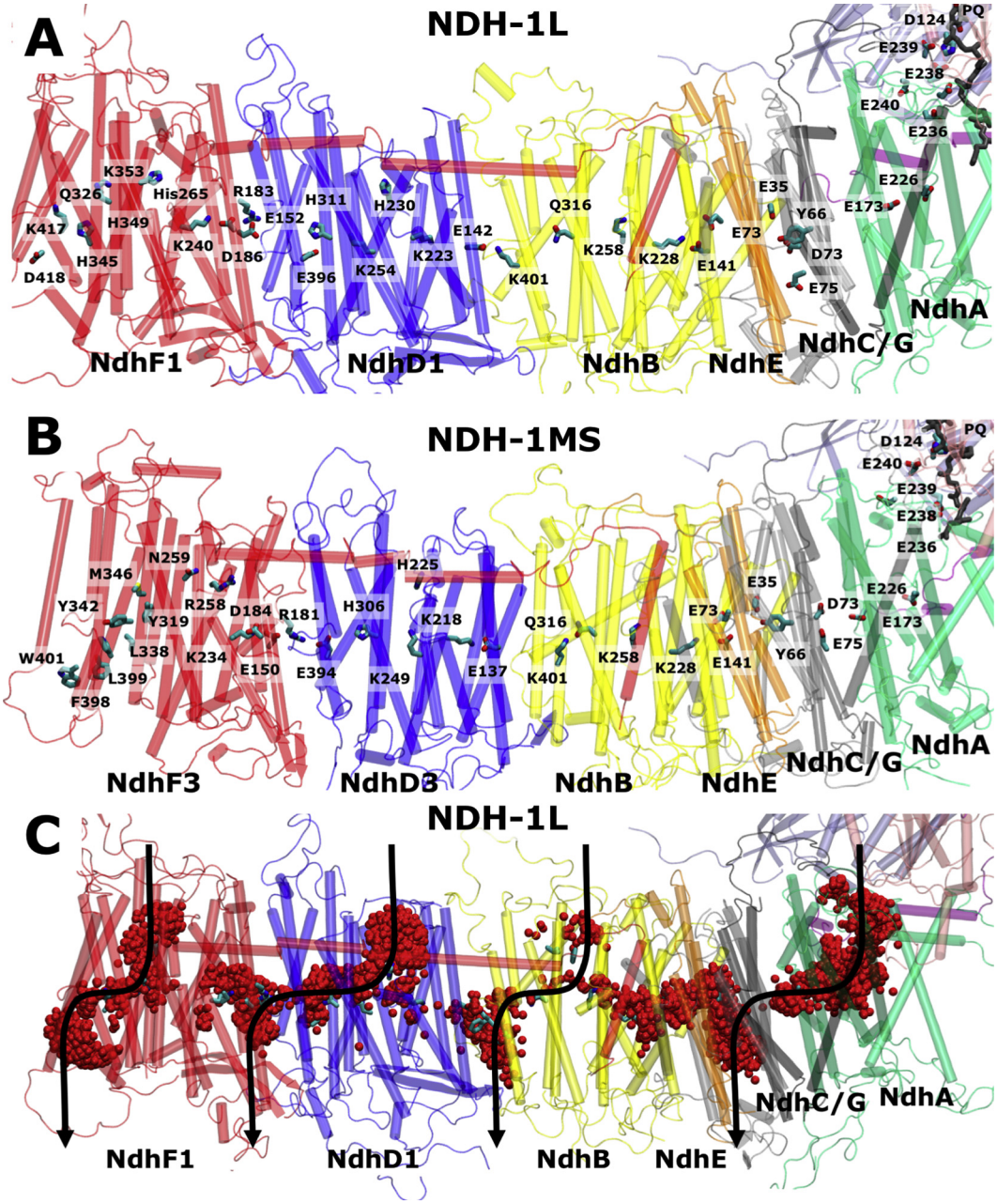

Fig. 3. The structure of the membrane domain of A) NDH-1L and B) NDH-1MS, showing an array of conserved buried polar/charged residues at the center of the membrane plane. The structure of NdhF3 contains several buried aromatic/hydrophobic residues. C) Hydration dynamics of proton channels in the NDH-1L isoform, showing the average water structure (in red) obtained during the MD simulations. The putative proton channels are marked with black arrows.

complex I [14,60,61].

During the MD simulations of the NDH-1L isoform, we observe that water molecules spontaneously enter the antiporter-like subunits NdhB, NdhD1, NdhF1, and NdhA from the cytoplasmic side at conserved buried lysine residues ($Lys353_F$/$Lys254_D$/$Lys258_B$), and provide conduits for protons via a Grotthuss-type mechanism to the buried protein interior, similar as in complex I [16,62,63]. The water molecules form hydrogen-bonded arrays via bridging histidine/glutamine residues ($His349_F$/$His345_F$; $His311_D$; $Gln316_B$) to terminal glutamate/lysine residues ($Lys417_F$/$Asp418_F$; $Glu396_D$; $Lys401_B$) that are connected to the luminal side of the membrane residues (Fig. 3, Table S3). The continuous hydrogen-bonded pathways are broken by a restriction site at conserved non-polar residues ($Phe352_F$/$Ile405_F$; $Phe393_D$/$Leu233_D$ $Phe398_B$/$Leu309_B$, Table S3), providing a possible gating element for the proton pumping machinery. Importantly, the observed proton channels form at symmetry-related locations, connected by a 180-degree rotation-translation symmetry, similar to the bacterial enzyme [16]. This strongly suggests that the proton channels are established at evolutionary conserved locations in complex I-like enzymes.

We also observe spontaneous hydration of NdhA from the cytoplasmic side to the buried glutamate quartet, comprising residues $Glu236_A$, $Glu226_A$, $Glu173_A$, and $Asp73_C$. The water arrays are further connected to the conserved $Tyr66_G$, a residue that was observed to undergo conformational changes in a recently resolved structure of mammalian complex I [14]. This proton channel connects to the luminal side at the NdhE/B interface via $Tyr66_G$, $Glu75_G$, and $Asp73_G$ (Fig. 4, see Table S3).

Each of the central lysine residues in the antiporter-like subunits are electrostatically wired to a conserved Glu/Lys ion-pair within the same subunit (Fig. 4). When this ion-pair is closed, the central lysine prefers a

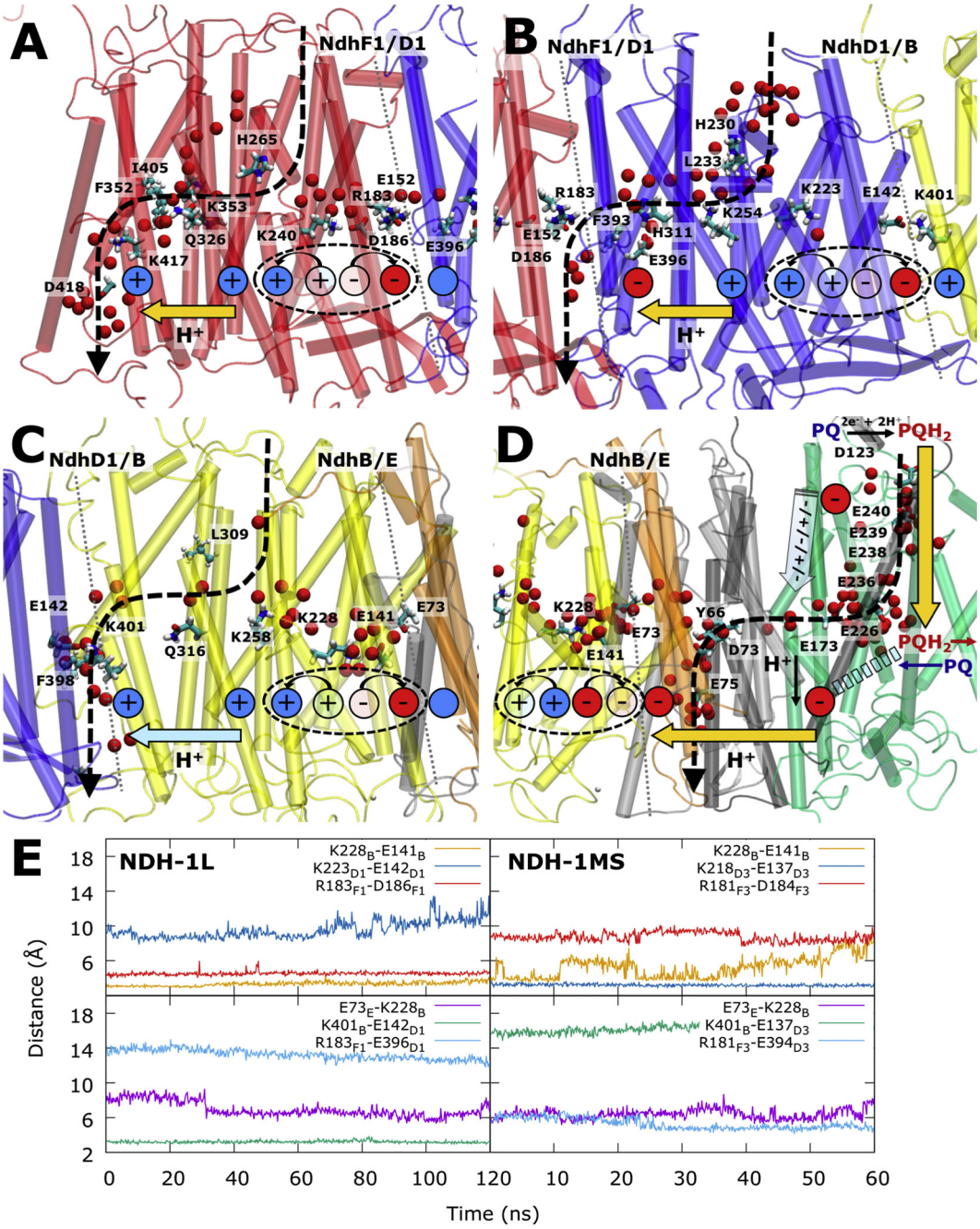

Fig. 4. Close-up of the proton channel in A) NdhF1, B) NdhD1, C) NdhB, and D) NdhA/C/G subunits of the NDH-1L model formed during MD simulations. E) Dynamics of the Glu/Lys ion-pairs within and between neighboring subunits in the NDH-1L (left) and NDH-1MS (right) models. For each subunit, it is schematically shown how opening of the Glu/Lys ion-pair triggers deprotonation of central lysine residue that pushes the proton horizontally via the terminal edge of the subunit (see text).

protonated state, which in turn favors hydration from the cytoplasmic side of the membrane [16,55]. In the MD simulations of the NDH1-1L/1MS models, the Glu/Lys ion-pair also form contacts with terminal residues of the neighboring subunits, which lowers the pK_a of the middle Lys due to electrostatic repulsion, and pushes the proton further towards to the terminal glutamate/lysine residues in TM12. Deprotonation of the middle lysine induces closing of the cytoplasmic channel due to the weaker electric field originating from the neutral residue. Accumulation of positive charge at the terminal edge of TM12 further induces opening of the next Glu/Lys ion pair of the neighboring subunit, which in turn mediates the electrostatic signal propagation across the complete membrane domain [15]. Our simulations suggest that the proton channels in NdhA/C are strongly coupled with plastoquinone-chemistry and dynamics, and further to the first Glu/Lys ion pair in NdhB, inducing its opening. The 80 Å-long HL-helix secures the electrostatic coupling between subunits remains strong by clamping the antiporter-like subunits together.

We also observe hydration of the putative proton channels in the NdhD3, NdhB, and NdhA/C subunits during MD simulations of the NDH-1MS isoform at locations similar to those in the NDH-1L isoform (Fig. S10). However, we do not observe clear proton output channels in the NdhA/C and NdhB subunits, possibly due to different conformation of the conserved Glu/Lys ion pairs (Fig. 4E) that are also likely to control the hydration dynamics [15]. Interestingly, the central polar/charged residues that form the proton channel in NdhF1 subunit are replaced by aromatic/aliphatic hydrophobic residues in the

corresponding NdhF3 subunit in NDH-1MS (see Fig. 3A, B). During the simulations, we observe stable buried channels in NdhF3 that could function as pathways for CO_2 to diffuse from the luminal side into the CupA/S subunits, or for the protons released in the hydration reaction to diffuse to the luminal side. Based on the sequence, CupA (CupB in NDH-1MS′) has a carbonic-anhydrase activity that catalyzes the conversion of CO_2 into bicarbonate (HCO_3^-) (Fig. S11) [64]. This ca. 430-residue subunit lacks structural templates, and binds to the smaller 130-residue CupS subunit that mediates NdhF/D-binding [65]. Our structural model of NdhF3 also contains a Glu/Lys ion-pair that is electrostatically coupled with the proton pumping machinery of the D3 subunit. It thus remains possible that this putative channel could open by a protonation signal that propagates across the membrane domain. The CupA/S-catalyzed hydration of CO_2 to HCO_3^-, releases protons at the cytoplasmic side that could be pumped across the membrane, and contribute to the formation of proton motive force (*pmf*). This process is expected to be thermodynamically driven by PQ reduction to PQH_2 as in the NDH-1L isoform.

4. Conclusions

We have presented here a structural model of two isoforms of the cyanobacterial NDH-1 complex that were derived based on experimentally resolved structures of the bacterial and mammalian respiratory complex I. The structural models of NDH-1 show a similar global architecture and conserved dynamics to the bacterial and mammalian respiratory enzymes. We identified how PQ binds near the N2 cluster and triggers coupled conformational and electrostatic transitions in the membrane domain upon formation of plastoquinol. We also identified a second transient PQ-binding site near the membrane domain that was suggested to couple with the proton pumping function. The NDH-1L isoform, which is involved in respiration and cyclic electron flow, shows formation of four putative proton channels at symmetry related locations. The structural architecture and dynamics support that protonation changes are controlled by flipping of conserved Glu/Lys ion-pairs that push the proton towards the terminal ends of the antiporter-like subunits, and propagate across the complete membrane domain. Our models suggest that the terminal subunit of the NDH-1MS complex lacks proton channels, but comprises residues that could form a gas channel for the CO_2-fixation process. Our work provides input for experimental validation of functional elements in NDH-1 and predicts that the core structural and functional features of NDH-1 resemble those of that have recently been derived for the respiratory complex I-family.

Transparency document

The Transparency document associated with this article can be found, in online version.

Acknowledgements

We thank Bill Rutherford, Natalia Battchikova, Eva-Mari Aro, Andrea Di Luca, and Ana P. Gamiz-Hernandez for insightful discussions. This work received funding from the European Research Council (ERC) under the European Union's Horizon 2020 research and innovation program/grant agreement 715311. The Leibniz-Rechenzentrum (LRZ) and Supermuc (grant: pr27xu) provided computational resources.

Author contributions

P.S. and V.R.I.K. designed research, P.S. performed research, P.S. and V.R.I.K. analyzed data, and P.S. and V.R.I.K. wrote the paper.

Competing interests

The authors declare no competing interests.

Appendix A. Supplementary data

Supplementary data to this article can be found online at https://doi.org/10.1016/j.bbabio.2018.11.010.

References

[1] N. Battchikova, M. Eisenhut, E.-M. Aro, Cyanobacterial NDH-1 complexes: novel insights and remaining puzzles, BBA-Bioenergetics 1807 (2011) 935–944, https://doi.org/10.1016/j.bbabio.2010.10.017.
[2] G. Peltier, E.-M. Aro, T. Shikanai, NDH-1 and NDH-2 plastoquinone reductases in oxygenic photosynthesis, Annu. Rev. Plant Biol. 67 (2016) 55–80, https://doi.org/10.1146/annurev-arplant-043014-114752.
[3] N. Battchikova, E.-M. Aro, P.J. Nixon, Structure and physiological function of NDH-1 complexes in cyanobacteria, in: G.A. Peschek, C. Obinger, G. Renger (Eds.), Bioenerg. Process. Cyanobacteria From Evol. Singul. to Ecol. Divers, Springer Netherlands, Dordrecht, 2011, pp. 445–467, , https://doi.org/10.1007/978-94-007-0388-9_16.
[4] Y. Munekage, M. Hashimoto, C. Miyake, K.I. Tomizawa, T. Endo, M. Tasaka, T. Shikanai, Cyclic electron flow around photosystem I is essential for photosynthesis, Nature 429 (2004) 579–582, https://doi.org/10.1038/nature02598.
[5] G.D. Price, M.R. Badger, F.J. Woodger, B.M. Long, Advances in understanding the cyanobacterial CO2-concentrating- mechanism (CCM): functional components, Ci transporters, diversity, genetic regulation and prospects for engineering into plants, J. Exp. Bot. 59 (2008) 1441–1461, https://doi.org/10.1093/jxb/erm112.
[6] F. Gao, J. Zhao, L. Chen, N. Battchikova, Z. Ran, E.-M. Aro, T. Ogawa, W. Ma, The NDH-1L-PSI supercomplex is important for efficient cyclic electron transport in cyanobacteria, Plant Physiol. 172 (2016) 1451–1464, https://doi.org/10.1104/pp.16.00585.
[7] L.N. Liu, Distribution and dynamics of electron transport complexes in cyanobacterial thylakoid membranes, BBA-Bioenergetics 1857 (2016) 256–265, https://doi.org/10.1016/j.bbabio.2015.11.010.
[8] R. Baradaran, J.M. Berrisford, G.S. Minhas, L.A. Sazanov, Crystal structure of the entire respiratory complex I, Nature 494 (2013) 443–448, https://doi.org/10.1038/nature11871.
[9] K. Fiedorczuk, J.A. Letts, G. Degliesposti, K. Kaszuba, M. Skehel, L.A. Sazanov, Atomic structure of the entire mammalian mitochondrial complex I, Nature 538 (2016) 406–410, https://doi.org/10.1038/nature19794.
[10] R.G. Efremov, L.A. Sazanov, Structure of the membrane domain of respiratory complex I, Nature 476 (2011) 414–421, https://doi.org/10.1038/nature10330.
[11] J. Zhu, K.R. Vinothkumar, J. Hirst, Structure of mammalian respiratory complex I, Nature 536 (2016) 354–358, https://doi.org/10.1038/nature19095.
[12] V. Zickermann, C. Wirth, H. Nasiri, K. Siegmund, H. Schwalbe, C. Hunte, U. Brandt, Mechanistic insight from the crystal structure of mitochondrial complex I, Science 347 (2015) 44–49, https://doi.org/10.1126/science.1259859.
[13] K.R. Vinothkumar, J. Zhu, J. Hirst, Architecture of mammalian respiratory complex I, Nature 515 (2014) 80–84, https://doi.org/10.1038/nature13686.
[14] A.N.A. Agip, J.N. Blaza, H.R. Bridges, C. Viscomi, S. Rawson, S.P. Muench, J. Hirst, Cryo-EM structures of complex I from mouse heart mitochondria in two biochemically defined states, Nat. Struct. Mol. Biol. 25 (2018) 1–9, https://doi.org/10.1038/s41594-018-0073-1.
[15] V.R.I. Kaila, Long-range proton-coupled electron transfer in biological energy conversion: towards mechanistic understanding of respiratory complex i, J. R. Soc. Interface 15 (2018) 20170916, , https://doi.org/10.1098/rsif.2017.0916.
[16] A. Di Luca, A.P. Gamiz-Hernandez, V.R.I. Kaila, Symmetry-related proton transfer pathways in respiratory complex I, Proc. Natl. Acad. Sci. U. S. A. 114 (2017) E6314–E6321, https://doi.org/10.1073/pnas.1706278114.
[17] V. Sharma, G. Belevich, A.P. Gamiz-Hernandez, T. Róg, I. Vattulainen, M.L. Verkhovskaya, M. Wikström, G. Hummer, V.R.I. Kaila, Redox-induced activation of the proton pump in the respiratory complex I, Proc. Natl. Acad. Sci. U. S. A. 112 (2015) 11571–11576, https://doi.org/10.1073/pnas.1503761112.
[18] A.P. Gamiz-Hernandez, A. Jussupow, M.P. Johansson, V.R.I. Kaila, Terminal electron-proton transfer dynamics in the quinone reduction of respiratory complex I, J. Am. Chem. Soc. 139 (2017) 16282–16288, https://doi.org/10.1021/jacs.7b08486.
[19] M. Wikström, V. Sharma, V.R.I. Kaila, J.P. Hosler, G. Hummer, New perspectives on proton pumping in cellular respiration, Chem. Rev. 115 (2015) 2196–2221, https://doi.org/10.1021/cr500448t.
[20] P. Prommeenate, A.M. Lennon, C. Markert, M. Hippler, P.J. Nixon, Subunit composition of NDH-1 complexes of *Synechocystis* sp. PCC 6803. Identification of two new ndh gene products with nuclear-encoded homologues in the chloroplast Ndh complex, J. Biol. Chem. 279 (2004) 28165–28173, https://doi.org/10.1074/jbc.M401107200.
[21] M. Shibata, H. Ohkawa, T. Kaneko, H. Fukuzawa, S. Tabata, A. Kaplan, T. Ogawa, Distinct constitutive and low-CO2-induced CO2 uptake systems in cyanobacteria: genes involved and their phylogenetic relationship with homologous genes in other organisms, Proc. Natl. Acad. Sci. U. S. A. 98 (2001) 11789–11794, https://doi.org/10.1073/pnas.191258298.
[22] M.L. Verkhovskaya, N.P. Belevich, L. Euro, M. Wikström, M.I. Verkhovsky, Real-

time electron transfer in respiratory complex I, Proc. Natl. Acad. Sci. U. S. A. 105 (2008) 3763–3767, https://doi.org/10.1073/pnas.0711249105.
[23] L.A. Sazanov, P. Hinchliffe, Structure of the hydrophilic domain of respiratory complex I from *Thermus thermophilus*, Science 311 (2006) 1430–1436, https://doi.org/10.1126/science.1123809.
[24] Z. He, F. Zheng, Y. Wu, Q. Li, J. Lv, P. Fu, H. Mi, NDH-1L interacts with ferredoxin via the subunit NdhS in *Thermosynechococcus elongatus*, Photosynth. Res. 126 (2015) 341–349, https://doi.org/10.1007/s11120-015-0090-4.
[25] J.G. Fedor, A.J.Y. Jones, A. Di Luca, V.R.I. Kaila, J. Hirst, Correlating kinetic and structural data on ubiquinone binding and reduction by respiratory complex I, Proc. Natl. Acad. Sci. U. S. A. 114 (2017) 12737–12742, https://doi.org/10.1073/pnas.1714074114.
[26] U. Brandt, Energy converting NADH: quinone oxidoreductase (complex I), Annu. Rev. Biochem. 75 (2006) 69–92, https://doi.org/10.1146/annurev.biochem.75.103004.142539.
[27] S.I. Maeda, M.R. Badger, G.D. Price, Novel gene products associated with NdhD3/D4-containing NDH-1 complexes are involved in photosynthetic CO_2 hydration in the cyanobacterium, *Synechococcus* sp. PCC7942, Mol. Microbiol. 43 (2002) 425–435, https://doi.org/10.1046/j.1365-2958.2002.02753.x.
[28] B. Webb, A. Sali, Comparative protein structure modeling using MODELLER, Curr. Protoc. Bioinformatics 54 (2016) 5.6.1–5.6.37, https://doi.org/10.1002/cpbi.3.
[29] F. Sievers, A. Wilm, D. Dineen, T.J. Gibson, K. Karplus, W. Li, R. Lopez, H. McWilliam, M. Remmert, J. Söding, J.D. Thompson, D.G. Higgins, Fast, scalable generation of high-quality protein multiple sequence alignments using Clustal Omega, Mol. Syst. Biol. 7 (2011), https://doi.org/10.1038/msb.2011.75.
[30] O.S. Smart, J.G. Neduvelil, X. Wang, B.A. Wallace, M.S.P. Sansom, HOLE: a program for the analysis of the pore dimensions of ion channel structural models, J. Mol. Graph. 14 (1996) 354–360, https://doi.org/10.1016/S0263-7855(97)00009-X.
[31] J. Huang, A.D. Mackerell, CHARMM36 all-atom additive protein force field: validation based on comparison to NMR data, J. Comput. Chem. 34 (2013) 2135–2145, https://doi.org/10.1002/jcc.23354.
[32] J.C. Phillips, R. Braun, W. Wang, J. Gumbart, E. Tajkhorshid, E. Villa, C. Chipot, R.D. Skeel, L. Kalé, K. Schulten, Scalable molecular dynamics with NAMD, J. Comput. Chem. 26 (2005) 1781–1802, https://doi.org/10.1002/jcc.20289.
[33] W. Humphrey, A. Dalke, K. Schulten, VMD: visual molecular dynamics, J. Mol. Graph. 14 (1996) 33–38, https://doi.org/10.1016/0263-7855(96)00018-5.
[34] A. Bakan, L.M. Meireles, I. Bahar, ProDy: protein dynamics inferred from theory and experiments, Bioinformatics 27 (2011) 1575–1577, https://doi.org/10.1093/bioinformatics/btr168.
[35] A. Di Luca, V.R.I. Kaila, Global collective motions in the mammalian and bacterial respiratory complex I, BBA-Bioenergetics 1859 (2018) 326–332, https://doi.org/10.1016/j.bbabio.2018.02.001.
[36] M. Babot, A. Galkin, Molecular mechanism and physiological role of active–deactive transition of mitochondrial complex I, Biochem. Soc. Trans. 41 (2013) 1325–1330, https://doi.org/10.1042/BST20130088.
[37] N.P. Belevich, G. Belevich, Z. Chen, S.C. Sinha, M.L. Verkhovskaya, Activation of respiratory complex I from *Escherichia coli* studied by fluorescent probes, Heliyon 3 (2017) e00224, , https://doi.org/10.1016/j.heliyon.2016.e00224.
[38] K. Parey, U. Brandt, H. Xie, D.J. Mills, K. Siegmund, J. Vonck, W. Kühlbrandt, V. Zickermann, Cryo-EM structure of respiratory complex I at work, elife 7 (2018), https://doi.org/10.7554/eLife.39213.
[39] H. Yamamoto, L. Peng, Y. Fukao, T. Shikanai, An Src homology 3 domain-like fold protein forms a ferredoxin binding site for the chloroplast NADH dehydrogenase-like complex in *Arabidopsis*, Plant Cell 23 (2011) 1480–1493, https://doi.org/10.1105/tpc.110.080291.
[40] N. Battchikova, L. Wei, L. Du, L. Bersanini, E.M. Aro, W. Ma, Identification of novel Ssl0352 protein (NdhS), essential for efficient operation of cyclic electron transport around photosystem I, in NADPH:plastoquinone oxidoreductase (NDH-1) complexes of *Synechocystis* sp. PCC 6803, J. Biol. Chem. 286 (2011) 36992–37001, https://doi.org/10.1074/jbc.M111.263780.
[41] H. Yamamoto, T. Shikanai, In planta mutagenesis of src homology 3 domain-like fold of ndhs, a ferredoxin-binding subunit of the chloroplast NADH dehydrogenase-like complex in arabidopsis, J. Biol. Chem. 288 (2013) 36328–36337, https://doi.org/10.1074/jbc.M113.511584.
[42] J. Zhao, F. Gao, J. Zhang, T. Ogawa, W. Ma, NdhO, a subunit of NADPH dehydrogenase, destabilizes medium size complex of the enzyme in *Synechocystis* sp. strain PCC 6803, J. Biol. Chem. 289 (2014) 26669–26676, https://doi.org/10.1074/jbc.M114.553925.
[43] C.C. Page, C.C. Moser, X. Chen, P.L. Dutton, Natural engineering principles of electron tunnelling in biological oxidation-reduction, Nature 402 (1999) 47–52, https://doi.org/10.1038/46972.
[44] S. De Vries, K. Dörner, M.J.F. Strampraad, T. Friedrich, Electron tunneling rates in respiratory complex I are tuned for efficient energy conversion, Angew. Chem. Int. Ed. 54 (2015) 2844–2848, https://doi.org/10.1002/anie.201410967.
[45] M. Verkhovskaya, M. Wikström, Oxidoreduction properties of bound ubiquinone in Complex I from *Escherichia coli*, BBA-Bioenergetics 1837 (2014) 246–250, https://doi.org/10.1016/j.bbabio.2013.11.001.
[46] N. Le Breton, J.J. Wright, A.J.Y. Jones, E. Salvadori, H.R. Bridges, J. Hirst, M.M. Roessler, Using HYPERFINE electron paramagnetic resonance spectroscopy to define the proton-coupled Electron transfer reaction at Fe-S cluster N2 in respiratory complex I, J. Am. Chem. Soc. 139 (2017) 16319–16326, https://doi.org/10.1021/jacs.7b09261.
[47] T. Yano, W.R. Dunham, T. Ohnishi, Characterization of the H^+-sensitive ubisemiquinone species (SQNf) and the interaction with cluster N2: new insight into the energy-coupled electron transfer in complex I, Biochemistry 44 (2005) 1744–1754, https://doi.org/10.1021/bi048132i.
[48] K. Zwicker, A. Galkin, S. Dröse, L. Grgic, S. Kerscher, U. Brandt, The redox-bohr group associated with iron-sulfur cluster N2 of complex I, J. Biol. Chem. 281 (2006) 23013–23017, https://doi.org/10.1074/jbc.M603442200.
[49] K. Tagawa, D.I. Arnon, Oxidation-reduction potentials and stoichiometry of electron transfer in ferredoxins, BBA-Bioenergetics 153 (1968) 602–613, https://doi.org/10.1016/0005-2728(68)90188-6.
[50] J. Warnau, V. Sharma, A. Gamiz-Hernandez, A. Di Luca, O. Haapanen, I. Vattulainen, M. Wikström, G. Hummer, V.R.I. Kaila, Redox-coupled quinone dynamics in the respiratory complex I, Proc. Natl. Acad. Sci. U. S. A. 115 (2018) E8413–E8420, https://doi.org/10.1073/pnas.1805468115.
[51] P.K. Sinha, J. Torres-Bacete, E. Nakamura-Ogiso, N. Castro-Guerrero, A. Matsuno-Yagi, T. Yagi, Critical roles of subunit NuoH (ND1) in the assembly of peripheral subunits with the membrane domain of *Escherichia coli* NDH-1, J. Biol. Chem. 284 (2009) 9814–9823, https://doi.org/10.1074/jbc.M809468200.
[52] M.L. Valentino, P. Barboni, A. Ghelli, L. Bucchi, C. Rengo, A. Achilli, A. Torroni, A. Lugaresi, R. Lodi, B. Barbiroli, M.T. Dotti, A. Federico, A. Baruzzi, V. Carelli, The ND1 gene of complex I is a mutational hot spot for Leber's hereditary optic neuropathy, Ann. Neurol. 56 (2004) 631–641, https://doi.org/10.1002/ana.20236.
[53] S. Okayama, Redox potential of plastoquinone A in spinach chloroplasts, BBA-Bioenergetics 440 (1976) 331–336, https://doi.org/10.1016/0005-2728(76)90067-0.
[54] M. Birungi, M. Folea, N. Battchikova, M. Xu, H. Mi, T. Ogawa, E.M. Aro, E.J. Boekema, Possibilities of subunit localization with fluorescent protein tags and electron microscopy examplified by a cyanobacterial NDH-1 study, BBA-Bioenergetics 1797 (2010) 1681–1686, https://doi.org/10.1016/j.bbabio.2010.06.004.
[55] A. Di Luca, M.E. Mühlbauer, P. Saura, V.R.I. Kaila, How inter-subunit contacts in the membrane domain of complex I affect proton transfer energetics, BBA-Bioenergetics 1859 (2018) 734–741, https://doi.org/10.1016/j.bbabio.2018.06.001.
[56] H. Wulfhorst, L.E. Franken, T. Wessinghage, E.J. Boekema, M.M. Nowaczyk, The 5 kDa protein NdhP is essential for stable NDH-1L assembly in *Thermosynechococcus elongatus*, PLoS One 9 (2014) e103584, , https://doi.org/10.1371/journal.pone.0103584.
[57] J. Zhao, W. Rong, F. Gao, T. Ogawa, W. Ma, Subunit Q is required to stabilize the large complex of NADPH dehydrogenase in *Synechocystis* sp. strain PCC 6803, Plant Physiol. 168 (2015) 443–451, https://doi.org/10.1104/pp.15.00503.
[58] M.M. Nowaczyk, H. Wulfhorst, C.M. Ryan, P. Souda, H. Zhang, W.A. Cramer, J.P. Whitelegge, NdhP and NdhQ: two novel small subunits of the cyanobacterial NDH-1 complex, Biochemistry 50 (2011) 1121–1124, https://doi.org/10.1021/bi102044b.
[59] J. Zhang, F. Gao, J. Zhao, T. Ogawa, Q. Wang, W.W. Ma, NdhP is an exclusive subunit of large complex of NADPH dehydrogenase essential to stabilize the complex in *Synechocystis* sp. strain PCC 6803, J. Biol. Chem. 289 (2014) 18770–18781, https://doi.org/10.1074/jbc.M114.553404.
[60] A. Jussupow, A. Di Luca, V.R.I. Kaila, How Cardiolipin Modulates the Structrue and Dynamics of Respiratory Complex I, (2018) (submitted).
[61] J.A. Letts, K. Fiedorczuk, L.A. Sazanov, The architecture of respiratory supercomplexes, Nature 537 (2016) 644–648, https://doi.org/10.1038/nature19774.
[62] V.R.I. Kaila, M. Wikstrom, G. Hummer, Electrostatics, hydration, and proton transfer dynamics in the membrane domain of respiratory complex I, Proc. Natl. Acad. Sci. U. S. A. 111 (2014) 6988–6993, https://doi.org/10.1073/pnas.1319156111.
[63] O. Haapanen, V. Sharma, Role of water and protein dynamics in proton pumping by respiratory complex I, Sci. Rep. 7 (2017) 7747, , https://doi.org/10.1038/s41598-017-07930-1.
[64] M.R. Badger, G.D. Price, CO_2 concentrating mechanisms in cyanobacteria: molecular components, their diversity and evolution, J. Exp. Bot. 54 (2003) 609–622, https://doi.org/10.1093/jxb/erg076.
[65] A. Korste, H. Wulfhorst, T. Ikegami, M.M. Nowaczyk, R. Stoll, NOE distance and dihedral angle restraints to calculate the solution structure of the NDH-1 complex subunit CupS from *Thermosynechococcus elongatus*, BBA-Bioenergetics 6 (2016) 249–252, https://doi.org/10.1016/j.dib.2015.12.004.